Heterojunction p-Cu2O/ZnO-n solar cell fabricated by spark plasma sintering

Christophe Tenailleau, Guillaume Salek, Thi Ly Le, Benjamin Duployer, Jean-Jacques Demai, Pascal Dufour, Sophie Guillemet-Fritsch

Mater Renew Sustain Energy (2017)6:18
DOI 10.1007/s40243-017-0102-8

BRIEF COMMUNICATION

Heterojunction p-Cu_2O/ZnO-n solar cell fabricated by spark plasma sintering

Christophe Tenailleau[1] · Guillaume Salek[1] · Thi Ly Le[1] · Benjamin Duployer[1] · Jean-Jacques Demai[1] · Pascal Dufour[1] · Sophie Guillemet-Fritsch[1]

Received: 21 April 2017 / Accepted: 27 August 2017

Abstract Cuprous oxide and zinc oxide nanoparticles were prepared at room temperature by inorganic polycondensation. X-ray diffraction (XRD) analyses show that the oxide phases formed are pure and well crystallized. The spark plasma sintering (SPS) technique was successfully used to prepare dense nanoceramics with superimposed layers of Cu_2O and ZnO nanopowders. Sintering conditions were optimized to densify the ceramics without phase transformation or diffusion. These ceramics were also characterized by XRD and scanning electron microscopy (SEM), as well as X-ray computed tomography (XCT). SEM and XCT showed that nanograins are preserved after SPS throughout both oxide materials, while a smaller layer (∼20 μm) of pure oxide phase with larger grains is formed in between Cu_2O and ZnO during the sintering process. The SPS technique results in high material density, with the absence of porosity and cracks, homogenous distribution, and a good phase separation. This is the first time that such as-prepared dense oxide-based heterojunction exhibits a photovoltaic effect under illumination opening a new route for preparing solar cells.

Keywords Copper oxide · Zinc oxide · Ceramics · Spark plasma sintering · X-ray tomography · Photovoltaics

Introduction

Solar cells are based on semi-conducting components that once assembled properly can convert efficiently sunlight into electricity. Silicon-based solar cells are still the most widely commercialized. However, other families of semiconducting materials (GaAs, CdTe, $CuInS_2$, and derivatives…) have long being studied and developed to obtain thin films that can facilitate solar energy conversion, miniaturization, and decrease costs. However, their toxicity and element scarcity are usually restricting factors for developing large-scale solar cells.

All-oxide photovoltaics constitute a promising generation of solar cells [1]. While n-type transparent conducting oxides are well reported (ZnO, TiO_2, In-Sn–O···), p-type semiconductors used in solar cells are often limited to Cu_2O [2–5]. However, the quantum yield for Cu_2O is yet to be improved with 6% conversion efficiency reached only recently [6], in comparison with the ∼20% theoretical value.

Solar cells based on p-Cu_2O/ZnO-n heterojunctions can be made by different techniques, mainly spin-coating and electrodeposition methods [7–9], magnetron sputtering [3, 4, 10], hydrothermal methods [11], from thermally activated metal sheets [12], or fabricated in air at low temperatures by atmospheric atomic layer deposition [13].

We have recently optimized a low-cost preparation process of crystalline oxide nanopowders that is applicable to a wide variety of structures and stoichiometries, including Cu_2O and ZnO materials [14]. Once dispersed in colloidal suspensions, the oxides can be integrated in thin-film solar cells.

These oxide nanopowders were used to produce dense layered nanoceramics by the spark plasma sintering (SPS) technique. To our knowledge, this is the first superimposed

✉ Christophe Tenailleau
tenailleau@chimie.ups-tlse.fr

[1] Centre Interuniversitaire de Recherche et d'Ingénierie des MATériaux (CIRIMAT) CNRS, INPT, UPS, Université de Toulouse, 118 route de Narbonne, 31062 Toulouse Cedex 09, France

Published online: 02 September 2017

ceramic of this type obtained in one step after sintering. Flash sintering of ZnO is well presented in the literature [15–18], while it is hard to find any detailed study on the sintering process of Cu_2O by SPS. Sintering Cu_2O by the conventional methods is very hard to perform without phase transformation. The SPS apparatus uses a pulsed current to heat very quickly a graphite die which contains the sample powder. This is a very interesting technique which allows to decrease considerably the time and temperature of a ceramic sintering process. It can also preserve the size of the raw nanopowders and nanograin size ceramics there obtained, so-called nanoceramics, can exhibit unusual physical properties (see [19, 20], for instance). High sample densifications (above 95%) were obtained after SPS treatments. The new p-type Cu_2O and n-type ZnO assembly created by SPS was characterized by X-ray diffraction (XRD) for phase crystalline states, scanning electron microscopy (SEM) for grains distribution essentially, and X-ray computed tomography (XCT) to probe the oxides interface and visualize the 3D volume in a non-destructive manner. This original p-Cu_2O/ZnO-n heterojunction was successfully tested as a solar cell.

Standard silicon-based solar cells are usually a few 100th of μm thick (complete Si cells are typically a few mm in thickness). Reduction of the silicon wafer thickness from its current value of about 180 μm to 10–20 μm would eliminate 90% of its effective costs. Multiple technologies exist, some of which have already demonstrated high efficiency on wafers as thin as 35 μm, including silicon grown epitaxially directly from vapor sources, silicon wafers produced directly from molten silicon without casting and wire sawing, and thinner wire saws. Thinner wafers also contribute to higher throughput processing, further reducing the costs. Specifically, the throughput of crystal growth, ingot cropping, wire sawing, and wet chemical steps are increased by having thinner wafers [21]. In wafer-based mono- and multi-crystalline Si solar cells, the absorption is routinely improved by texturing the surface with micrometre-sized pyramid-shaped features, which increase scattering of light into the cell, and by a silicon nitride anti-reflection coating. This approach is not practical for thin-film silicon solar cells, where the absorber layer thickness is on the order of 1–3 μm. In these cells, absorption is improved by properly engineered sub-micrometre surface texture, which enhances both light scattering into a thin absorber layer and the anti-reflection effect at the interfaces over a broad range of wavelengths and incident angles [22].

Most optimized, high-performance, bulk heterojunction solar cells have an active layer thickness of about 100 nm. However, the thin active layer of bandgap >2 eV is unfavorable for optical absorption and film coating. Thicker films can have higher performances [23]. A 20 μm free-standing Cu_2O layer was grown by thermal oxidation of copper foils and showed a 1.6 mA/cm^{-2} shift of current density at 0 Volt (i.e., J_{sc} value) [24]. Here, this is the first all-oxide ~300 μm-thick solar cell ever reported, to our knowledge. A few issues related to charge recombination and oxide conductivities are still to be answered. High material densification due to SPS treatment, compactness, low activation energies at small grain boundaries for both phases, and well-defined interfaces can explain these results. In addition, SPS treatment under vacuum or argon can reduce the oxide components, generating higher concentration of vacancies and improving the number of charges.

Experimental

Our simple synthesis method of metal oxide nanopowders used at low temperature without any organic and complexing agent allowed the preparation of pure crystalline Cu_2O and ZnO nanopowders [14]. Briefly, metal salts are dissolved in water in stoichiometric proportions. Solutions are then mixed with a large volume of lithium hydroxide and stirred for half an hour at ambient atmosphere. The addition of dilute ascorbic acid to the copper di-hydroxide

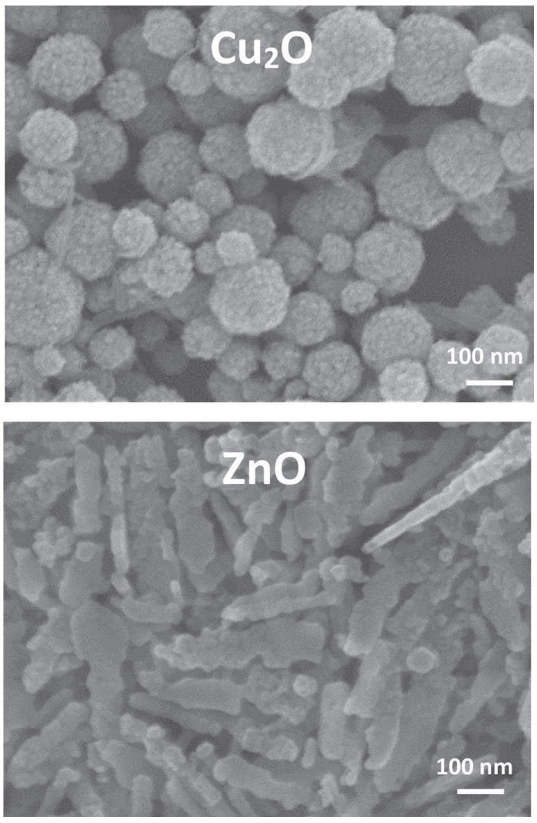

Fig. 1 Scanning electron microscopy images of the cuprite Cu_2O (*top*) and zinc oxide ZnO (*bottom*) nanoparticles after synthesis by inorganic polycondensation

formed after the previous stage is required to form Cu_2O. After washing with water, oxide nanoparticles of controlled size and morphology were isolated. The aqueous solvent is finally changed to ethanol and colloidal suspensions, which are stable for a few months in an azeotrope solution, can be used for thin films preparation by the dip-coating process.

For the first time to our knowledge, the co-sintering of Cu_2O and ZnO was possible in a short time ($\sim$30 min) by SPS using a Dr Sinter 2080 device from Sumitomo coal mining (Fuji Electronic Industrial, Saitama, Japan) with both phases being preserved as such after the experiment. 300 mg of oxide powders were used. A papyex layer (200 μm in thickness of C graphite) was put at both ends in the main graphite die (8 mm in diameter) to avoid contamination of the pistons. High vacuum and argon gas were used to avoid phase transformation. A pressure of 5kN (100 MPa) was applied to the sample from the beginning of the heating time and up to 800 °C (highest temperature tested, which was reached in 8 min, and a constant dwell time of 6 min at high temperature). Cooling was done at the furnace rate with the pressure released upon cooling. The pellet density was determined by the Archimedes method using an ARJ-220-4M balance (KERN, Murnau-Westried, Germany).

X-ray diffraction (XRD) data were recorded on a Bruker D4-ENDEAVOR diffractometer using a CuKα wavelength radiation (40 kV, 40 mA) and collected over the $10° < 2\theta < 100°$ range at room temperature, with a 0.02° step scan and 3.6 s/step.

Scanning electron microscopy (SEM) and back scattering electron microscopy (BSEM) were performed using a JEOL JSM6400 operated from 0.2 to 40 kV, with a resolution of 3.5 nm and 10 nm at 35 kV in SEI and BEI modes, respectively. The microscope is equipped with an Oxford INCA Energy Dispersive X-ray (EDX) Spectrometer for elemental and cartography analysis.

Two- and three-dimensional images were obtained by X-ray computed tomography (XCT) on a few mm^3 of ceramics with a Phoenix/GE Nanotom 180 using a tungsten target. The VG Studio Max 2.1 software was used for data visualization and process. Different XCT parameters were tested to verify their effects on the reconstructed images and to improve the characterization of the materials microstructure of similar diffusion factors. Typically, data measurement conditions were: Zero Mode (2.7 W power for an optimal resolution in between 1.8 and 60 μm), $U = 90$ kV, $I = 160$ μA, source/objet distance = 7.6 mm, source/detector distance = 250 mm, voxel size = 1.5 μm, step time = 1500 ms, and five images averaged/step, while the first two images were skipped to avoid image reminiscence after each rotation. 1440 images were recorded after 360° sample rotation.

I–V measurements were carried out with a BENTHAM PV 300 from ES instrument using a xenon source (150 W) and a halogen quartz source (100 W) to cover the whole sunlight spectrum for photovoltaic characterization in standard conditions (298 K, 1000 W/m^2, AM1.5). The PV 300 system from Bentham/ES (ref. IL-DUAL-Xe/QH & 605) is specifically dedicated to efficiency measurements in standard conditions on small areas for different types of solar cells. A reference LP-Si-CAL-Ex silicon photodiode was used for the system calibration in between 300 and 1100 nm before efficiency measurements.

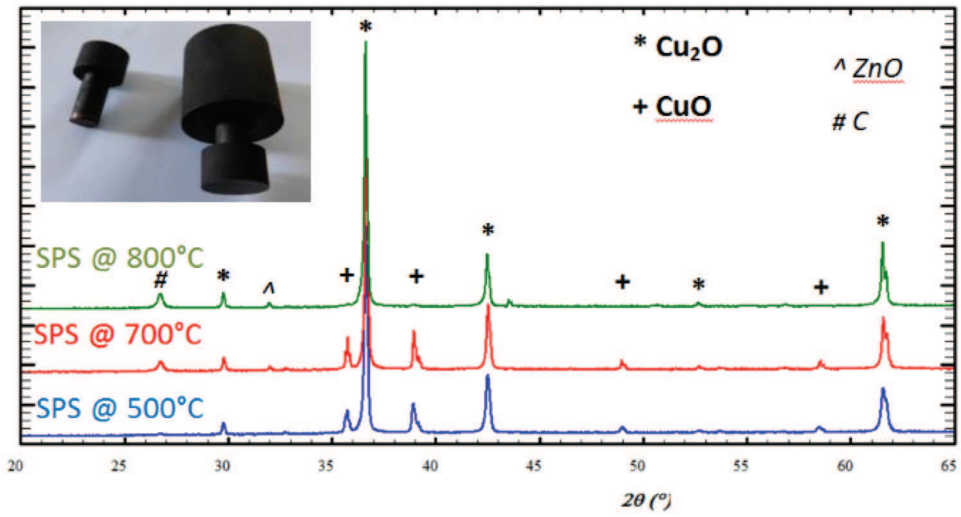

Fig. 2 Room-temperature X-ray diffraction patterns of superimposed Cu_2O/ZnO nanoceramics prepared by SPS. Inset shows the graphite sample holder used for SPS treatment

Results and discussion

Recently, we have optimized a simple synthetic approach to prepare crystalline nanopowders of oxides at low costs [14, 25]. This soft-chemistry method was used to prepare Cu_2O and ZnO nanopowders of controlled size and morphology. Cu_2O nanoparticles are spherical (100 nm average size in diameter), while ZnO nanorods ($\sim$50 nm in width and 300 nm in length) can be prepared using a solvent mixture of 30 vol% of ethanol in water (Fig. 1). These nanopowders were favorably associated to form a dense nanoceramic (densification > 95%) after sintering at 500–800 °C using the SPS technique. The papyex layers were removed by polishing on both sides and the final pellet thickness was about 300 μm. X-ray diffraction patterns, recorded on the cuprite-side of the pellets at room temperature, show that Cu_2O and CuO phases are present after SPS treatments and heating at 500 and 700 °C in argon atmosphere (Fig. 2). ZnO is also seen by XRD. At 800 °C, CuO is not present and the only oxide phase observed is Cu_2O, while a very small quantity of Cu metal starts to form due to the reducing atmosphere provided by the graphite environment (see the 8 mm in diameter matrix and pistons used for SPS in inset of Fig. 2).

The pellet showing only Cu_2O and ZnO phases by XRD was fully characterized. SEM images show that nanoparticles are well preserved after SPS treatments (Fig. 3). No coexistence of the phases was determined and a net separation was observed showing a good compatibility of those materials essentially due to the fast sintering process and close oxide phase dilatation parameters. However, a smaller interface ($\sim$20 μm thick) is clearly evidenced on secondary electron microscopy and back-scattered images. This interface is composed of larger grains of the ZnO phase as evidenced by EDX analyses (see Fig. 3). This abrupt change in grain sizes was already observed in ZnO-based systems sintered by flash sintering and attributed to the occurrence of electric-potential-induced abnormal grain growth [15]. This enhanced grain growth and/or coarsening would be associated with the accumulation of electrons and formation of cation vacancies at ZnO grain boundaries and free surfaces due to particular electrical potentials.

The perpendicular orientation to the electrode support is usually more favorable for faster charge conduction. Rod-like structures facilitate penetration and effective interfacial area, which normally result in reduced charge carrier path length and increased photovoltaic parameters. However, a nanocrystalline porous ZnO film constructed from upright-standing nanosheets with the *c* axis parallel to the substrate and incorporated into a dye sensitized solar cell (or DSSC) indicated the highest level of efficiency due to this specific morphology [26]. In our case, SEM images show that nanorods-like particles are randomly distributed

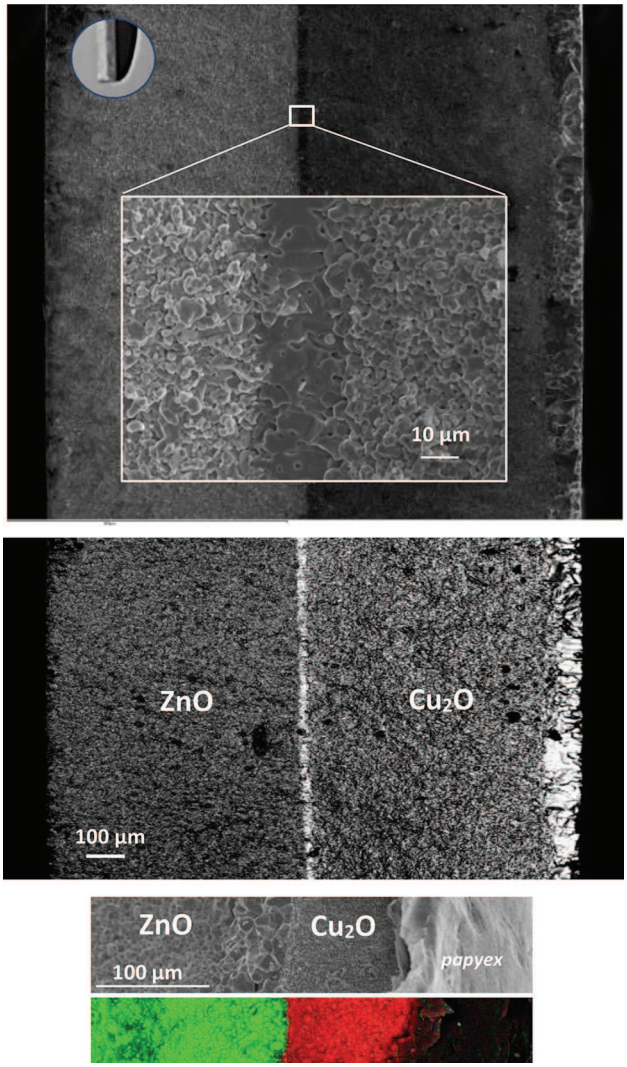

Fig. 3 Scanning secondary (*top*) and back-scattered (*middle*) electron microscopy images of the Cu_2O/ZnO heterojunction. *Inset* is a photo of the nanoceramic obtained after SPS treatment. EDX mapping analysis results are given at the bottom image, showing that the interlayer of larger grains consists mainly of ZnO

throughout the layer after SPS sintering. The charge transport (electrons in the n-type ZnO semi-conducting layer) is, therefore, favorable within each nanoparticle along both longitudinal and perpendicular directions with high ceramic densification.

Advances in characterization techniques are always pushing further the comprehension of the materials' chemical formation/transformation and physical properties. Recently, X-ray computed tomography has been developed to probe and visualize inside the matter in a non-destructive manner. Indeed, with the XCT technique, it is now possible to obtain a large set of 2D images of the inner core of a material and use these to reconstruct the 3D volume. Depending on the XCT technique and beam source (X-ray,

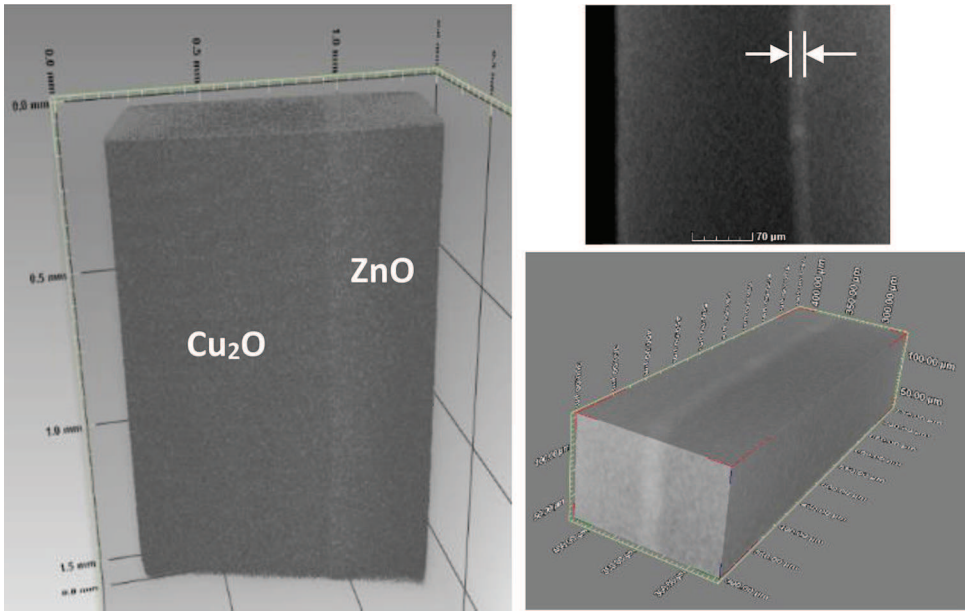

Fig. 4 2D/3D images obtained by laboratory X-ray computed tomography on Cu_2O/ZnO nanoceramics. The interlayer is emphasized by *arrows*

neutron or electron, essentially), it is now usually possible to detect variable phases, cracks, defects… without any damages of a sample, from a few hundreds of micrometers down to a few nanometers. XCT data information can give valuable microstructural information and reach a wide community of scientists. Dense and thick materials with high atomic numbers are hard to characterize at a high resolution with conventional XCT lab instruments. It is usually necessary to minimize the sample size for valuable data reconstruction. Another difficulty arises when material phases contrast is lowered due to close atomic numbers and/or compositions, such as Cu_2O and ZnO. However, we managed to record 2D and 3D images of our nanoceramics and separate both phases. We could also distinguish clearly, by XCT, the intermediate phase of larger granulometry (and probably different density) at the oxide interface (Fig. 4). No cracks were seen throughout the whole studied volumes, especially at the phase separation. Therefore, not only the high densification of the nanoceramics was confirmed by XCT measurements, but also the two oxide phases of close density and diffusion factors could be separated over a large material volume.

Thin films of gold (~50 nm in thickness) were deposited on both sides of the ceramic composite, with only ~1 mm-diameter spot on the ZnO side for the light to illuminate a maximum of sample. *I–V* curves were measured in dark and under sunlight in standard conditions. The nanoceramic obtained after SPS treatment showed a photovoltaic behavior under sunlight illumination (Fig. 5). This is the first time, to our knowledge, that a solar cell is made by this technique. The absolute value of the short-circuit current density J_{sc} is of 10 nA cm^{-2} and the open-circuit voltage V_{oc} ~ 0.07 V. These values are still very low, but the preparation method is very promising for industrial applications.

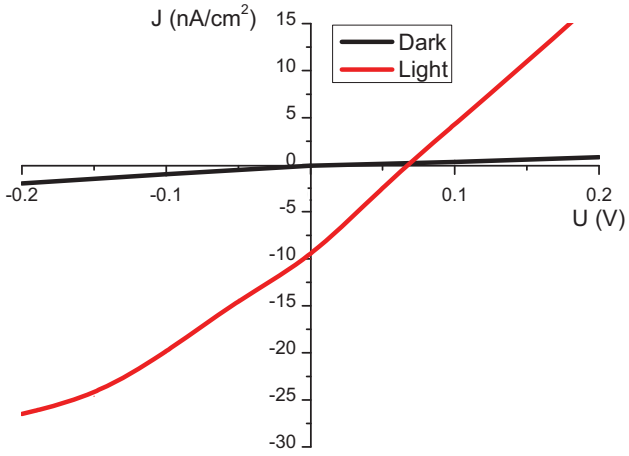

Fig. 5 *I–V* curves in the dark and under standard solar irradiance (AM1.5 and 1000 W/m^2 at room temperature) on the oxide-based heterojunction Cu_2O/ZnO solar cell obtained by SPS showing a photovoltaic effect. Scale units are 0.5 mm (left), 70 µm (*top right*), and 50 µm (*bottom right*)

Sinsermsuksakul et al. recently observed some signs of a large positive conduction band offset CBO (a small positive CBO is desirable to reduce interface recombination without any loss in photo-current collection) in a thicker SnS-based solar cell (>500 nm), including a dark/light *J–V* cross over, higher diode voltage (i.e., V_{oc}), small fill factor (FF), and low J_{sc} [27]. This CBO discrepancy may be because of a variation of the SnS surface condition for different film thicknesses due to preferred and anisotropic crystal orientations of SnS during film preparation.

Garnett and Yang demonstrated in 2010 strong light-trapping properties of nanowire arrays, which improve the conversion efficiency of Si solar cells. Their 5 μm nanowire arrays' radial p–n junction solar cells fabricated from 8 and 20 μm Si absorbing layers achieved conversion efficiencies of 4.8 and 5.3%, respectively, under AM1.5 illumination. The significant light-trapping effect, above the theoretical limit for a randomizing system, indicates that there might be photonic improvement effects [28].

The efficiency was found to increase as the oxide film thickness decreases in a Cu_2O/Cu heterojunction, up to a limiting thickness of 26.30 μm after which the efficiency decreases with decrease in the oxide film thickness, depending essentially on the oxidation conditions (with $T \sim 1000$ °C, time = 3 min) found for Cu_2O and Cu, with $I_{sc} = 518$ μA and $V_{oc} = 86.0$ mV [29].

An increasing J_{sc} value was also measured as a function of the increasing Cu_2O thickness for TiO_2/Cu_2O all-oxide heterojunction solar cells entirely produced by spray pyrolysis onto fluorine-doped tin oxide (FTO) covered glass substrates [30].

In addition, enhanced photovoltaic effect was reported in 2013 in the ferroelectric lanthanum-modified lead zirconate titanate (PLZT) [31]. PLZT ceramics were prepared by hot-pressing calcinations at 1240 °C under 40 MPa pressure. Both sides of the 1 cm in diameter resulting pellets were then polished down to about 300 μm in thickness before metal deposition (~100 nm thick, by radio-frequency magnetron sputtering). The photovoltaic response of PLZT capacitor was expanded from ultraviolet to visible spectra and may have important impact on design and fabrication of high-performance photovoltaic devices. These preparation technique and ceramic thickness are comparable to those described here.

The final sample thickness after SPS process is a limitation to the search for very thin materials. The technique usually requires a few mm-thick powder sample to insert in the graphite die to obtain compact material with good mechanical strength. Then, samples down to ~100 μm in thickness can be obtained after careful polishing. However, it depends on the nature and grain size of the raw powder. For instance, self-supporting ceramic materials having a reduced thickness (below 100 μm) and containing metal oxides were produced straight from the SPS [32].

Further investigations are currently being undertaken to deeply characterize the nanoceramic microstructure and optimize its photovoltaic properties. The oxide layer thickness and compactness, the nature of electrodes, and quality of interfaces can probably enhance the conversion efficiency. These results could open up a new route for preparing future generations of solar cells.

Conclusions

A solar cell was produced using the spark plasma sintering process. The heterojunction formed and studied in this paper was composed of two oxide phases, Cu_2O and ZnO. First, pure crystalline nanopowders of Cu_2O and ZnO were synthesized by a simple soft-chemistry method. These powders were then inserted on top of each other into a graphite die to prepare a junction of the two oxides. The SPS technique allows to obtain a nanoceramic with high densification for a very short time of heat treatment under high pressure. The oxide phases remain well fitted and separated after SPS treatment, while a limited region of grain growth is observed on the ZnO side at the oxide interface probably due to an electrical potential in the SPS apparatus. Finally, the solar energy conversion into electricity was tested with success on this system, showing that this method can be used to prepare photovoltaic devices.

Acknowledgements The French FERMaT Midi-Pyrénées Federation FR3089 is deeply acknowledged for providing X-ray tomography laboratory facility. Mr Geoffroy Chevallier is thanked for assistance in the SPS treatments. This work was supported by the French Ministry of Education and Research and the Vietnamese government with the University of Sciences and Technology in Hanoi (USTH).

References

1. Rühle, S., Anderson, A.Y., Barad, H.-N., Kupfer, B., Bouhadana, Y., Rosh-Hodesh, E., Zaban, A.: All-oxide photovoltaics. J. Phys. Chem. Lett. **3**, 3755–3764 (2012)
2. Musa, A.O., Akomolafe, T., Carter, M.J.: Production of cuprous oxide, a solar cell material, by thermal oxidation and a study of its physical and electrical properties. Solar Energy Mater. Solar Cells **51**, 305–316 (1998)
3. Akimoto, K., Ishizuka, S., Yanagita, M., Nawa, Y., Goutam, K., Sakurai, T.: Thin film deposition of Cu_2O and application for solar cells. Sol. Energy **80**, 715–722 (2006)
4. Chen, J.W., Perng, D.C., Fang, J.F.: Nano-structured Cu_2O solar cells fabricated on sparse ZnO nanorods. Solar Energy Mater. Solar Cells **95**, 2471–2477 (2011)
5. Wong, T.K.S., Zhuk, S., Masudy-Panah, S., Dalapati, G.K.: Current status and future prospects of copper oxide heterojunction solar cells. Materials **9**, 271–292 (2016)
6. Minami, T., Nishi, Y., Miyata, T.: Heterojunction solar cell with 6% efficiency based on an n-type aluminum–gallium–oxide thin film and p-type sodium-doped Cu_2O sheet. Appl. Phys. Express **8**, 022301–022304 (2015)
7. Oku, T., Yamada, T., Fujimoto, K., Akiyama, T.: Microstructures and photovoltaic properties of Zn(Al)O/Cu_2O-based solar cells

prepared by spin-coating and electrodeposition. Coatings **4**, 203–213 (2014)
8. Jeong, S.S., Mittiga, A., Salza, E., Masci, A., Passerini, S.: Electrodeposited ZnO/Cu_2O heterojunction solar cells. Electrochim. Acta **53**, 2226–2231 (2008)
9. Katayama, J., Ito, K., Matsuoka, M., Tamaki, J.: Performance of Cu_2O/ZnO solar cell prepared by two-step electrodeposition. J. Appl. Electrochem. **34**, 687–692 (2004)
10. Herion, J., Niekisch, E.A., Scharl, G.: Investigation of metal oxide/cuprous oxide heterojunction solar cells. Sol. Energy Mater. **4**, 101–112 (1980)
11. Wei, J., Hailiang, D., Junfu, Z., Suihu, D., Zhuxia, Z., Tianbao, L., Xuguang, L., Bingshe, X.: p-Cu_2O/n-ZnO heterojunction fabricated by hydrothermal method. Appl. Phys. A **109**, 751–756 (2012)
12. Minami, T., Miyata, T., Nishi, Y.: Efficiency improvement of Cu_2O-based heterojunction solar cells fabricated using thermally oxidized copper sheets. Thin Solid Films **559**, 105–111 (2014)
13. Levskayaan, Y., Hoyea, R.L.Z., Sadhanalab, A., Musselmanb, K.P., MacManus-Driscoll, J.L.: Fabrication of ZnO/Cu_2O heterojunctions in atmospheric conditions: improved interface quality and solar cell performance. Solar Energy Mater. Solar Cells **135**, 43–48 (2015)
14. Salek, G., Tenailleau, C., Dufour, P., Guillemet-Fritsch, S.: Room temperature inorganic polycondensation of oxide (Cu_2O and ZnO) nanoparticles and thin films preparation by the dip-coating technique. Thin Solid Films **589**, 872–876 (2015)
15. Zhang, Y., Jung, J.-I., Luo, J.: Thermal runaway, flash sintering and asymmetrical microstructural development of ZnO and ZnO–Bi_2O_3 under direct currents. Acta Mater. **94**, 87–100 (2015)
16. Beynet, Y., Izoulet, A., Guillemet-Fritsch, S., Chevallier, G., Bley, V., Pérel, T., Malpiece, F., Morel, J., Estournès, C.: ZnO-based varistors prepared by spark plasma sintering. J. Eur. Ceram. Soc. **35**, 1199–1208 (2014)
17. Ning, J.L., Jiang, D.M., Kim, K.H., Shim, K.B.: Influence of texture on electrical properties of ZnO ceramics prepared by extrusion and spark plasma sintering. Ceram. Int. **33**, 107–114 (2007)
18. Schmerbauch, C., Gonzalez-Julian, J., Roder, R., Ronning, C., Guillon, O.: Flash sintering of nanocrystalline zinc oxide and its influence on microstructure and defect formation. J. Am. Ceram. Soc. **97**, 1728–1735 (2014)
19. Guillemet-Fritsch, S., Valdez-Nava, Z., Tenailleau, C., Lebey, T., Durand, B., Chane-Ching, J.Y.: Colossal permittivity in ultrafine grain size $BaTiO_{3-x}$ and $Ba_{0.95}La_{0.05}TiO_{3-x}$ materials. Adv. Mater. **20**, 551–555 (2008)
20. Bordeneuve, H., Tenailleau, C., Guillemet-Fritsch, S., Smith, R., Suard, E., Rousset, A.: Structural variations and cation distributions in $Mn_{3-x}Co_xO_4$ ($0 \leq x \leq 3$) dense ceramics using neutron diffraction. Solid State Sci. **12**, 379–386 (2010)
21. Berney Needleman, D., Poindexter, J.R., Kurchin, R.C., Peters, I.M., Wilson, G., Buonassisi, T.: Economically sustainable scaling of photovoltaics to meet climate targets. Energy Environ. Sci. **9**, 2122 (2016)
22. Mailoa, J.P., Seog Lee, Y., Buonassisi, T., Kozinsky, I.: Textured conducting glass by nanosphere lithography for increased light absorption in thin film solar cells. J. Phys. D Appl. Phys. **47**, 085105 (2014)
23. Yin, H., Cheung, S.H., Ngai, J.H.L., Ho, C.H.Y., Chiu, K.L., Hao, X., Li, H.W., Cheng, Y., Tsang, S.W., So, S.K.: Thick-film high-performance Bulk-Heterojunction solar cells retaining 90% PCEs of the optimized thin film cells. Adv. Electron. Mater. **3**(4), 1700007 (2017). doi:10.1002/aelm.201700007
24. Wilson, S., Xiang, C., Tolstova, Y., Lewis, N.S., Atwater, H.A.: Thin free-standing Cu_2O substrates via thermal oxidation for photovoltaic devices, 978-1-4673-0066-7/12, IEEE Journal (2011) 003191
25. Salek, G., Dufour, P., Guillemet-Fritsch, S., Tenailleau, C.: Sustainable low temperature preparation of $Mn_{3-x}Co_xO_4$ ($0 \leq x < 3$) spinel oxide colloidal dispersions used for solar absorber thin films. Mater. Chem. Phys. **162**, 252–262 (2015)
26. Hosono, E., Fujihara, S., Honma, I., Zhou, H.: The fabrication of an upright-standing zinc oxide nanosheets for use in dye sensitized solar cells. Adv. Mater. **17**, 2091–2094 (2005)
27. Sinsermsuksakul, P., Hartman, K., Bok Kim, S., Heo, J., Sun, L., Hejin Park, H., Chakraborty, R., Buonassisi, T., Gordon, R.G.: Enhancing the efficiency of SnS solar cells via band-offset engineering with a zinc oxysulfide buffer layer. Appl. Phys. Lett. **102**, 053901 (2017)
28. Garnett, E., Yang, P.: Light trapping in silicon nanowire solar cells. Nano Lett. **10**, 1082–1087 (2010)
29. Ohajianya, A.C., Abumere, O.E.: Effect of cuprous oxide (Cu_2O) film thickness on the efficiency of the copper-cuprous oxide (Cu_2O/Cu) solar cell. Int. J. Eng. Sci. **2**, 42–47 (2013)
30. Pavan, M., Rühle, S., Ginsburg, A., Keller, D.A., Barad, H.-N., Sberna, P.M., Nunes, D., Martins, R., Anderson, A.Y., Zaban, A., Fortunato, E.: TiO_2/Cu_2O all-oxide heterojunction solar cells produced by spray pyrolysis. Solar Energy Mater. Solar Cells **132**, 549–556 (2015)
31. Zhang, J., Su, X., Shen, M., Dai, Z., Zhang, L., He, X., Cheng, W., Cao, M., Zou, G.: Enlarging photovoltaic effect: combination of classic photoelectric and ferroelectric photovoltaic effects. Sci Rep **3**, 2109 (2013)
32. Ansart, F., Estournes, C., Lenormand, P., Rieu, M., Zahid, M.: Patent: production of self-supporting ceramic materials having a reduced thickness and containing metal oxides, 23rd FR 2946979 and PCT WO/2010/146311, EIFER-UPS, EdF (2010)